Effect of double aluminium doping on the structure, stability and electronic properties of small gold clusters

ARTICLE *in* JOURNAL OF MATERIALS SCIENCE · JULY 2015

Impact Factor: 2.37 · DOI: 10.1007/s10853-015-9007-z

3 AUTHORS:

Debajyoti Bhattacharjee

Tezpur University

15 PUBLICATIONS **68** CITATIONS

SEE PROFILE

Bhupesh Kumar Mishra

D. N. Government College, Itanagar, Arunac…

45 PUBLICATIONS **279** CITATIONS

SEE PROFILE

Ramesh C Deka

Tezpur University

99 PUBLICATIONS **1,015** CITATIONS

SEE PROFILE

J Mater Sci
DOI 10.1007/s10853-015-9007-z

Effect of double aluminium doping on the structure, stability and electronic properties of small gold clusters

Debajyoti Bhattacharjee[1] · Bhupesh Kr. Mishra[2] · Ramesh Ch. Deka[1]

Received: 12 February 2015 / Accepted: 1 April 2015

Abstract In this work, we have used density functional theory with PW91PW91 functional to analyse the structures, relative stabilities and electronic properties of small bimetallic neutral and charged Au_nAl_2 ($n = 1$–5) clusters. The results reveal that doping with two Al atoms can significantly affects the geometries of the ground-state Au_{n+2} ($n = 1$–5) clusters. The relative stabilities of the clusters were investigated on the basis of average binding energies, fragmentation energies and second-order difference of energies. The electronic properties are calculated using vertical ionization potential, vertical electron affinity values and these parameters show even–odd alternation phenomenon. The nature of bonding interaction is also investigated for the first time in Al-doped clusters using Bader's quantum theory of atoms in molecules which indicates the presence of covalent bonding in the studied clusters. The population analysis reveals the transfer of electrons from Al to Au atoms which is responsible for the enhance stability of doped clusters.

Electronic supplementary material The online version of this article (doi:10.1007/s10853-015-9007-z) contains supplementary material, which is available to authorized users.

✉ Ramesh Ch. Deka
ramesh@tezu.ernet.in

[1] Department of Chemical Sciences, Tezpur University, Napaam 784 028, Assam, India

[2] Department of Chemistry, D. N. Govt. College, Itanagar 791113, Arunachal Pradesh, India

Introduction

Bimetallic clusters find wide importance in recent days because their structures and properties are usually different from the monometallic clusters. By adjusting the element components of bimetallic clusters, their properties could be well modulated. In bimetallic clusters, the doped pure metals often exhibit more favourable properties for applications than the non-doped pure metals. Among the different metal clusters, pure and doped gold clusters have received considerable attention because of their physical and chemical properties, and also due to their various potential applications in the fields of materials science, optics, solid state chemistry, nanotechnology, catalysis and biological science, in recent years [1–12]. Due to these reasons, a large number of theoretical and experimental studies were carried out by many groups to investigate the structural and electronic properties of gold monometallic as well as bimetallic nanoclusters [13–21]. Li et al. systematically analysed the equilibrium geometries, relative stabilities and electronic and magnetic properties of anionic Au_nMg ($n = 1$–8) clusters and found that lowest energy structures for the Mg-doped clusters are different to that of the bare Au clusters with $[Au_3Mg]^-$ cluster that has the most enhanced chemical stability [22]. Applying DFT, Wang et al. studied the Cu-doped Au clusters and compared them with pure Au clusters. Their results reveal that for neutral and anionic clusters, the structures are planar for both bare- and Cu-doped Au clusters. But in case of cationic clusters, a transition from 2D to 3D occurs at Au_6Cu^+ [23]. Kyasu et al. performed anion photoelectronic study on Au_nM^- ($n = 2$–7), M = Pd, Ni, Zn, Cu and Al, clusters [24]. They explored that for the binary clusters containing Pd, Ni and Cu, their valence electrons are shared with those of the Au clusters, whereas for Al the

Published online: 21 April 2015

doped atom is weakly bound to Au clusters. In addition to single metal-doped Au clusters, lots of studies are also carried out on doubly doped gold clusters. Jun et al. performed DFT to the low-lying isomers of Au_nY_2 ($n = 1$–4) clusters [25]. They reveal that the gold–yttrium interaction is strong enough to modify the growth pattern of bare gold clusters. In a previous study, we also investigated the structural property and stability of both single and double Be-doped gold clusters and found that the doped atom can tremindously effect the stability and structure of pure clusters [26].

When we consider aluminium, it is a member of boron family and third most abundant element as well as most abundant metal in the earth. The study of the geometric and electronic properties of nanoclusters composed of Au and Al atoms found importance in recent days both for theoretical reasons and for their potential applications in the field of nanotechnology. Till now, a few studies on aluminium-doped gold clusters have been already carried out. Bouwen et al. produced bimetallic Au_nAl_m clusters by a dual-target dual-laser vaporization source [27]. They differentiate different bimetallic clusters in terms of different cluster geometries dependent on the nature of the dopant atoms. Heinebrodt et al. studied bimetallic Au–Al clusters using time-of-flight mass spectrometer [28]. Their results suggested that each aluminium atom contributes three electrons to the common potential well, as expected for a simple trivalent metal. Using DFT, Wang et al. performed theoretical study on anionic Au_nAl^- ($1 \leq n \leq 8$) clusters [29]. Similarly, Xia et al. studied the Au_nAl ($n = 1$–13) clusters [30] and Majumdar et al., investigated the Au_5Al clusters [31]. These studies reveal that doping of single Al can affect the stability and structural properties of bare Au clusters. If we consider the double Al-doped gold clusters, to the best of our knowledge, no systematic theoretical investigations into Al_2Au_n clusters have been performed. Therefore, it is both natural and promising for us to investigate the properties of doubly Al-doped Au clusters. Therefore, by applying DFT, we studied the structural and electronic properties of neutral as well as charged Au clusters doped with two Al atoms, Au_nAl_2 ($n = 1$–5). In this study, we optimized a certain type of structures by doping Al atoms at different positions in the bare Au clusters. The importance of this work lies in the fact that nanosized Au clusters already show tremendous catalytic activity for different types of reactions and doping of a metal like Al can further enhanced its catalytic property. The novelty of the work with reference to the previous works lies in the facts that for the first time we have studied all the neutral and charged clusters for two Al metal-doped Au clusters and compared with the pure ones. Also for the first time, we have performed QTAIM study in the Al-doped Au clusters to study the bond parameters. Therefore, our present study can provide powerful platform to consider the Al-doped Au clusters in the further experimental research.

Computational details

We generated the initial structures in neutral state using classical simulated annealing method with the help of Forcite Plus code as encoded in the MATERIAL STUDIO software [32]. The Universal force field (UFF) [33] which was already proved to be reliable for gold-based systems [34, 35] was adopted to perform this simulation. The cut-off radius was chosen to be 15.5 °A and a NVE ensemble was used. A total of 100 annealing structures were generated at high temperature (1000 K) and 50 heating ramps per cycle. The less energetic i.e., the most stable structure obtained by this simulation was used as the input for further DFT calculations.

For geometry optimizations and frequency analysis of Au_nAl_2 clusters, we have used DFT-based gradient-corrected exchange and correlation functional of Perdew–Wang (PW91PW91) [36] to explore the stationary points on the potential energy surface. Since, relativistic effects play a key role in the structure and energetic of Au-containing clusters, we used the Los Alamos LANL2DZ [37, 38] effective core pseudopotentials (ECP) and valence double-ζ basis sets for Au. The Al atoms are treated with 6–311 + G(d) basis set. PW91PW91 functional is used successfully in the study of previous Al-doped Au clusters [29, 30] as well as studies on other metal clusters also [15, 39, 40]. Full geometry optimizations have been performed for the neutral and charged clusters without imposing any symmetry constraints. In order to obtain the lowest energy-doped isomers, initial structures were constructed substituting Au atoms by Al atoms in the pure gold structures at various attaching sites. The vibrational frequencies for all the structures are found to be positive confirming them to be at energy minima. The zero-point vibrational energy corrections have been included in all the calculations. All the calculations are carried out using GAUSSIAN 09 suits of programme [41]. The total energies of the most stable clusters are used to determine their binding energy, relative stability, ionization potential, electron detachment energy as well as electron affinity as a function of clusters size to describe the stability and electronic properties of the clusters. To investigate the nature of bonding in the studied clusters, we have relied upon Bader's quantum theory of atoms in molecules (QTAIM) [42–44]. For QTAIM analysis, we have generated the wave function using Gaussian 09 at the same level of theory as employed in structure optimization and then used the AIMALL package [45] to study different bond parameters.

Results and discussion

Structural study of Au_nAl_2 clusters

Figures 1–3 represent the various lowest energy structures for neutral and charged Au_n and Au_nAl_2 clusters. Among various isomers obtained for a particular cluster, the energy of the most stable isomer is taken as zero and energy of the others are compared relative to it.

Neutral clusters

The optimized structures for neutral clusters are depicted in Fig. 1. To study the doped clusters, we first optimized the bare Au clusters which are in good agreement with the previous study [13]. For the doped clusters, the most stable cluster for $AuAl_2$ is 1(1a) of triangular shape. The Au–Al bond length here is 2.545 Å which is in accordance with previous study on Al-doped gold clusters (2.419 Å) [30].

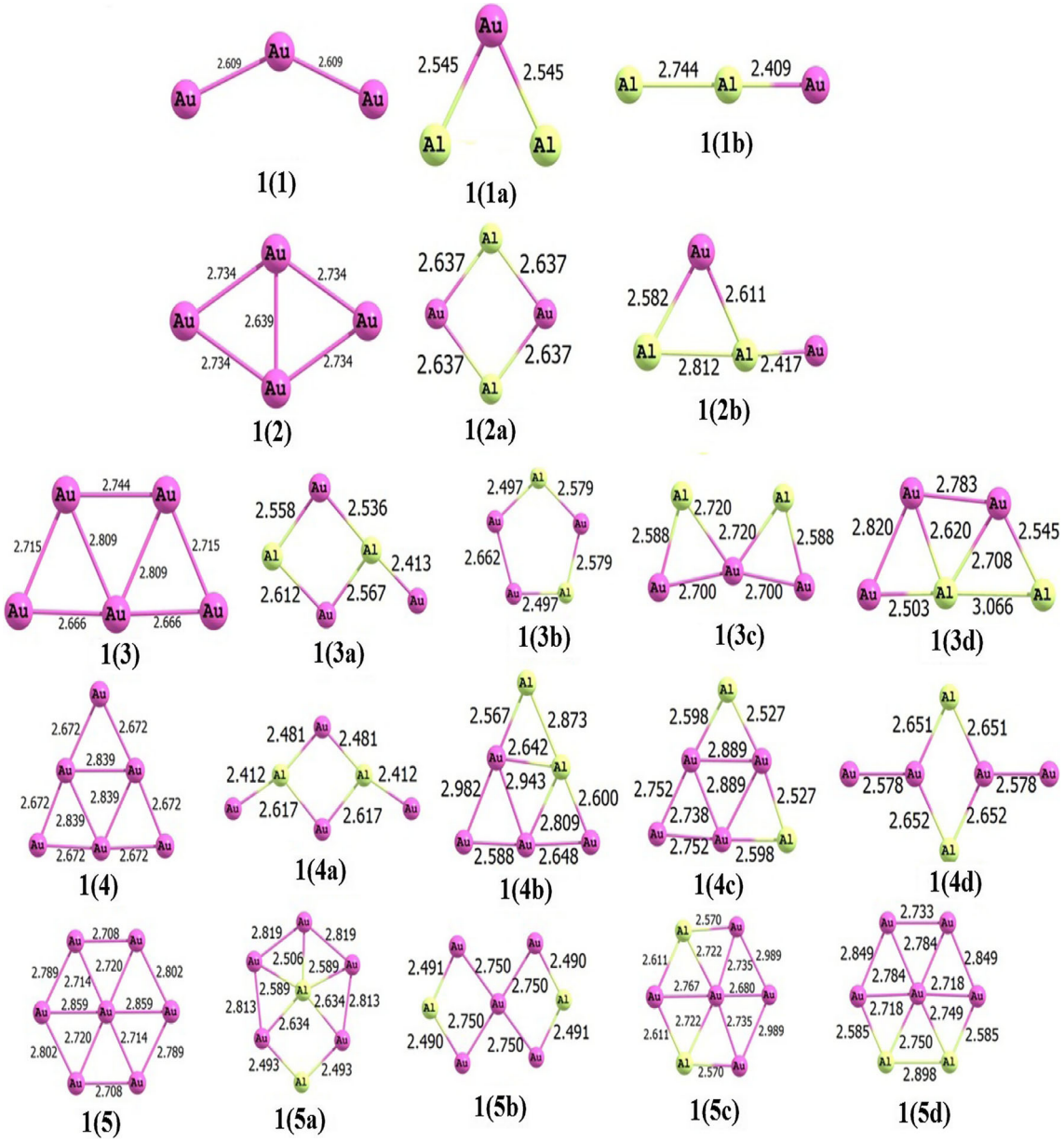

Fig. 1 Optimized structures of neutral Au_{n+2} and Au_nAl_2 ($n = 1$–5) clusters

The isomer 1(1b) is higher in energy compared to 1(1a) by 0.51 eV. In case of Au_2Al_2, the lowest energy isomer is 1(2a) having square planar geometry with Au–Al bond length of 2.637 Å. The other isomer is found to be higher in energy by 0.18 eV. Next cluster is Au_3Al_2 where the most stable isomer is 1(3a) having shortest Au–Al bond length of 2.413 Å. For Au_4Al_2, the most stable isomer is 1(4a) having shortest Au–Al bond length of 2.412 Å. This bond length is in close agreement with previous reported data of 2.35 Å for single Al-doped Au clusters [31]. Finally, for Au_5Al_2 cluster, we obtained a stable isomer 1(5a) having the same geometry as the bare counterpart. Here, the calculated value of shortest Au–Al bond length is found to be 2.506 Å.

This study on neutral-doped clusters points out that all the isomers have planar structure i.e., no any 3D isomer exists. This is in contrast to the study on single Al-doped Au clusters [30, 46] where 3D isomers are observed in most of the clusters. Apart from $n = 2$ and 5, all the most stable isomers for double Al-doped clusters have different geometries compared to the pure clusters. However, there exists at least one isomer for all the clusters where the pure and doped clusters have similar geometry. These facts suggest that the doubly doped Al atoms can affect the geometries of the ground state of neutral Au_n clusters.

Charged clusters

The optimized structures for the charged clusters are shown in Fig. 2 and 3 for the cationic and anionic clusters, respectively. For cationic $AuAl_2^+$ clusters, we get only one type of isomer 2(1a) by replacing the Au atoms with Al atoms at different positions. The isomer is found to be bent in shape with Au–Al bond length of 2.604 Å. For $Au_2Al_2^+$ cluster, the most stable isomer is 2(2a) having the same square planar geometry as the Au counterpart. The other isomer 2(2b) is found to be higher in energy to 2(2a) by 0.74 eV. For the rest of the clusters, the lowest energy isomers are found to be 2(3a), 2(4a), and 2(5a) for $Au_3Al_2^+$, $Au_4Al_2^+$ and $Au_5Al_2^+$, respectively (Fig. 2). Here we obtained a 3D isomer 2(3a) for $n = 3$ indicating a deviation from planarity of the clusters at this point. However, for the rest of the clusters, no any 3D isomers are observed. In case of anionic clusters, the most stable isomers are found to be 3(1a), 3(2a), 3(3a), 3(4a) and 3(5a) for $AuAl_2^-$, $Au_2Al_2^-$, $Au_3Al_2^-$, $Au_4Al_2^-$ and $Au_5Al_2^-$, respectively (Fig. 3). For the most stable $Au_2Al_2^-$ cluster, the shortest Au–Al bond length of 2.472 Å is comparable with that of 2.48 Å as reported by Wang et al. [29]. For anionic clusters, also a transition from 2D to 3D structure is observed at $n = 3$.

From this study on charged clusters, it can be seen that in contrast to neutral clusters, charged clusters show a deviation from planarity. For the cationic clusters, apart from $n = 2$ and 5, all the most stable isomers have different geometry to that of the bare clusters. On the other hand, only the most stable isomers for $n = 1$ and 4 have same geometry to that of the pure clusters. This indicates that for charged clusters also doping of two Al atoms can play a key role to effect the geometries of the ground state Au_n clusters and the effect seems to be higher than that of the neutral clusters.

Stability of Au_nAl_2 clusters

We have calculated the relative stabilities of the Au_nAl_2 clusters in terms of averaged binding energies per atom, (E_b) fragmentation energies, ΔE, and second-order difference of energies, $\Delta^2 E$, using formulae (1–7) given below. All these three parameters already established to be powerful tools to reflect the relative stability of the clusters.

For Au_n clusters averaged binding energies $E_b(Au_{n+2})$, fragmentation energies $\Delta E(Au_{n+2})$, and second-order difference of energies $\Delta^2 E(n)$ are calculated using the following formulae:

$$E_b(Au_{n+2}) = [(n+2)E(Au) - E(Au_{n+2})]/(n+2) \quad (1)$$

$$E_b(Au_{n+2})^q = [E(Au)^q + nE(Au) - E(Au_{n+2})^q]/(n+2) \quad (2)$$

$$\Delta E(Au_{n+2})^q = [E(Au_{n+1})^q + E(Au) - E(Au_{n+2})^q] \quad (3)$$

$$\Delta^2 E(Au_{n+2})^q = [E(Au_{n+1})^q + E(Au_{n+3})^q - 2E(Au_{n+2})^q] \quad (4)$$

where $E(Au)$ represents the ground state energy of the Au, q is the charge on the cluster, $q = 0$, $+1$ and -1 for neutral, cationic and anionic clusters, respectively, and n is the number of gold atoms associated with the clusters.

On the other hand, for Au_nAl_2 clusters, averaged binding energies $E_b(n)$, fragmentation energies $\Delta E(n)$, and second-order difference of energies $\Delta^2 E(n)$ are calculated using the following formulae:

$$E_b(Au_nAl_2)^q = [2E(Al)^q + nE(Au) - E(Au_nAl_2)^q]/(n+2) \quad (5)$$

$$\Delta E(Au_nAl_2) = [E(Au_{n-1}Al_2) + E(Au) - E(Au_nAl_2)^q] \quad (6)$$

$$\Delta^2 E(Au_nAl_2)^q = \left[E(Au_{n-1}Al_2) + E(Au_{n+1}Al_2) - 2E(Au_nAl_2)^q\right] \quad (7)$$

where $E(Al_2Au_n)$, $E(Au)$ and $E(Al)$ represent the total energy of the Al_2Au_n, Au and Al, respectively.

Binding energies per atom

Figure 4 represents the variation of calculated binding energies per atom (E_b) for the most stable isomers as a

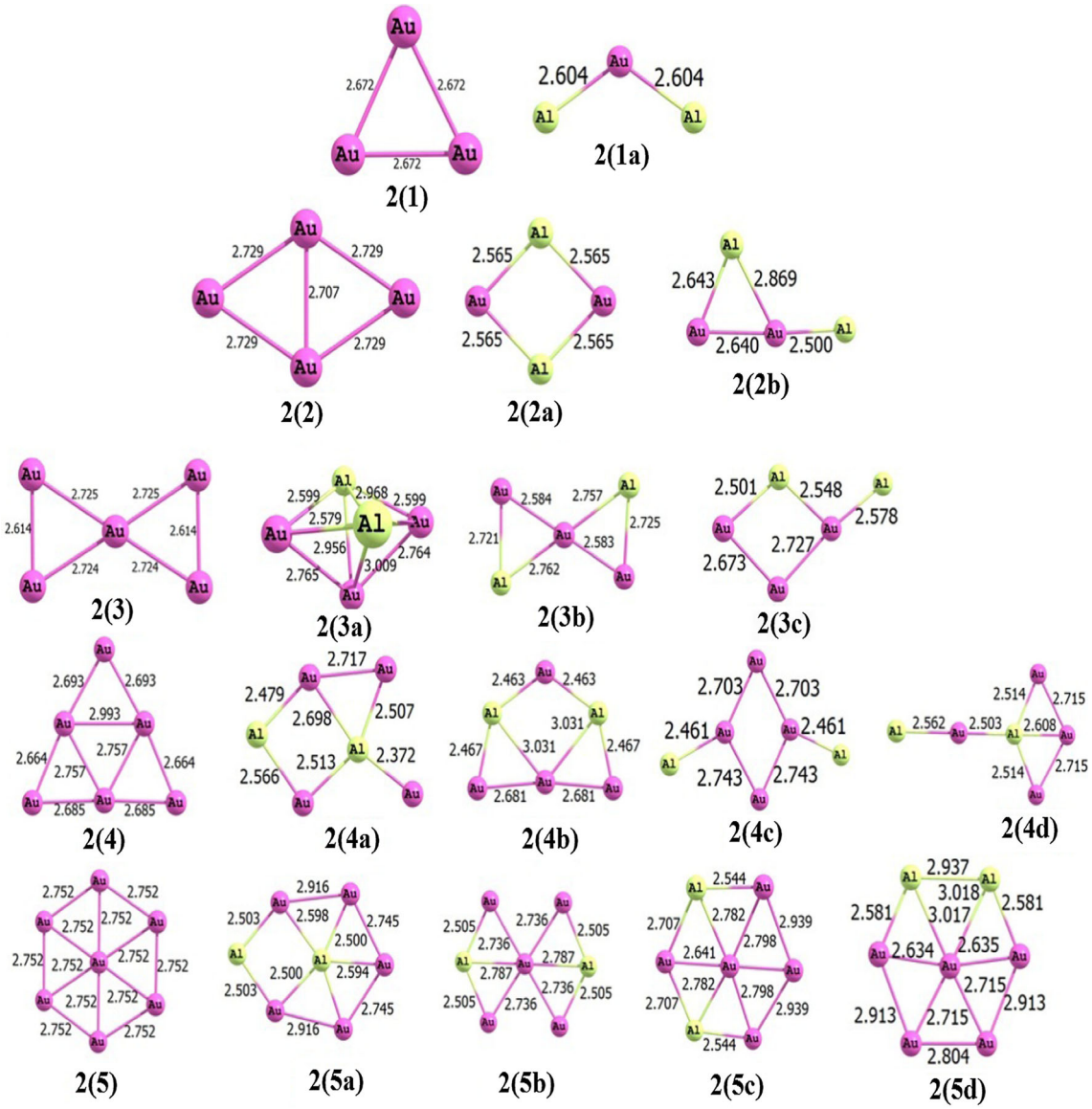

Fig. 2 Optimized structures of cationic Au_{n+2} and Au_nAl_2 ($n = 1$–5) clusters

function of cluster size. The binding energies of the doped clusters relative to pure gold clusters are compared here. The figure indicates that the binding energy per atom for pure clusters increases with cluster size for the neutral clusters which means that the clusters continue to gain energy during the growth process. In case of charged clusters, the B.E. values show an even–odd alternation. For neutral- and anionic-doped clusters, the graphs show sharp peaks at $n = 4$ and 3, respectively, indicating the higher stability of these clusters in the region $n = 1$–5. For the cationic-doped clusters, the E_b values decrease with cluster size. From the plots, it can be clearly understand that binding energy values for doped clusters are considerably higher than that of the pure clusters. Thus, the doped clusters have enhanced stability in all the neutral, cationic and anionic clusters in comparison to the bare Au clusters. For neutral and anionic clusters, the variation of B.E. is found to be similar to that of the single-doped clusters [29, 30, 46]. On comparing the binding energies of charge and neutral clusters (Fig. S1 of supplementary information), the binding energy order is found to be increases as neutral < anionic < cationic for Al-doped clusters. This order is identical to that of the doubly Be- and Mg-doped Au clusters as reported in our previous studies [26, 47].

Fragmentation energies

Fragmentation energy is the quite sensitive quantity that reflects the relative stability of cluster that can be observed in mass abundance spectra. The variation of values of

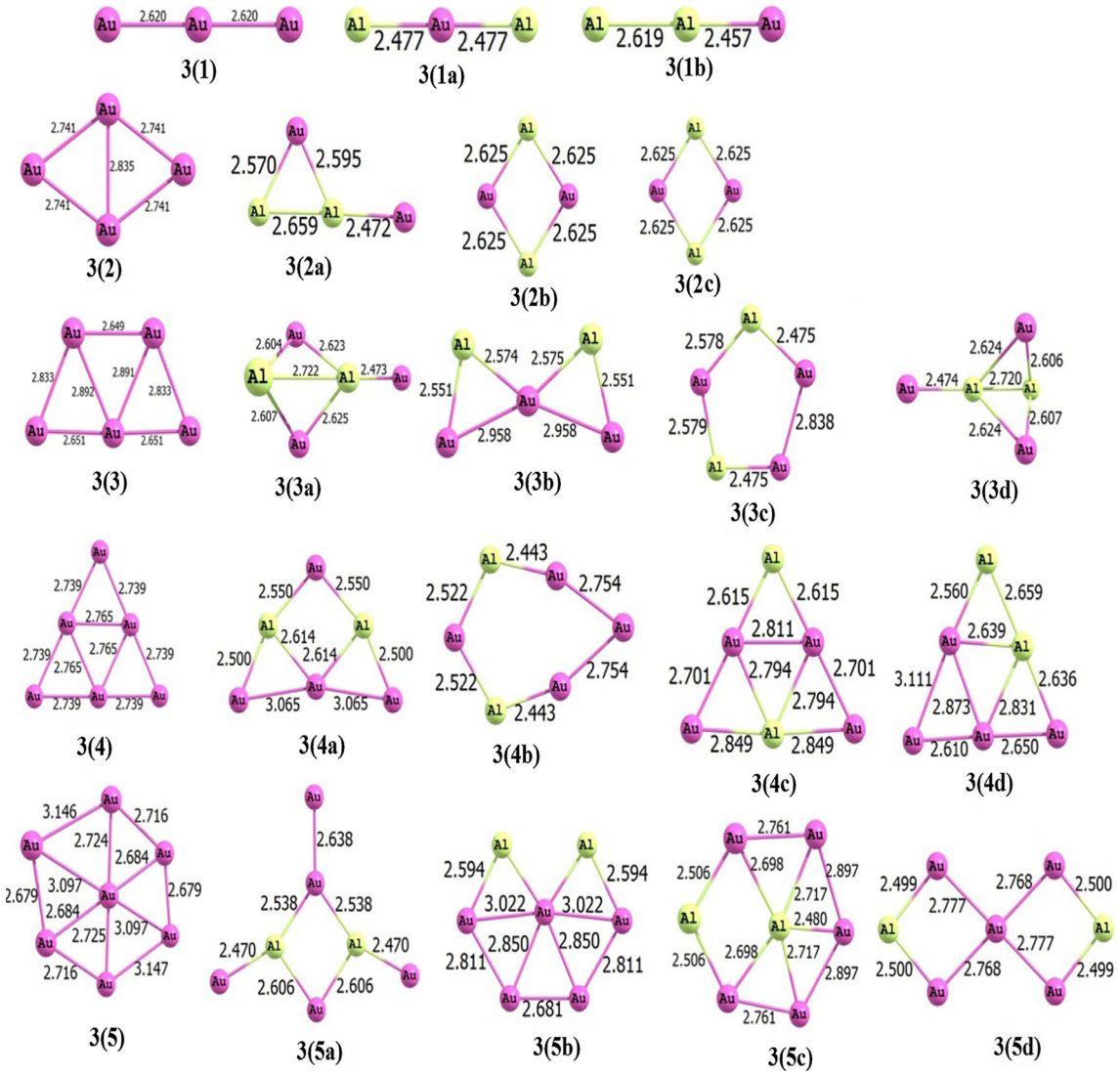

Fig. 3 Optimized structures of anionic Au_{n+2} and Au_nAl_2 ($n = 1$–5) clusters

fragmentation energies for the most stable Au- and Al-doped clusters as a function of cluster size is shown in Fig. 5. The figure indicates that both the bare as well as doped clusters exhibit even–odd alternation with respect to cluster size. For neutral clusters, $Au_{4,6}$ and $Au_{2,4}Al$ clusters have higher stability indicating that clusters with even number of atoms are more stable than that with odd number of atoms. However, for the charged clusters, the odd numbered clusters are seemed to be more stable. The neutral and anionic Au_nAl_2 clusters follow almost the same trend as observed for bare clusters. Also the variation of plots in these two types of clusters is identical with that of the singly doped clusters [29, 46]. For neutral and anionic clusters, a sharp peak occurs at $n = 2$, whereas for cationic clusters, sharp peaks occur at $n = 2$ and 5 indicating the stability of these clusters in the region $n = 1$–5.

Second-order difference of energies

The variation of second-order difference of energies (Δ^2E) for the most stable Au- and Al-doped clusters as a function of cluster size is depicted in Fig. 6. The second-order difference of energies (Δ^2E) provide the relative stability of a cluster of size n with respect to its neighbour. From Fig. 6, it can be reveal that bare as well as doped clusters exhibit the even–odd alternation. For neutral clusters, the curve shows a peak at $n = 2$ indicating its higher stability. In case of charged clusters, the curves have sharp peaks at $n = 2$ and 3 for cationic and anionic clusters, respectively, indicating the stability of the clusters at these points. The variation of the plots for neutral and anionic clusters is found to be similar with that of singly Al-doped Au clusters [29, 46].

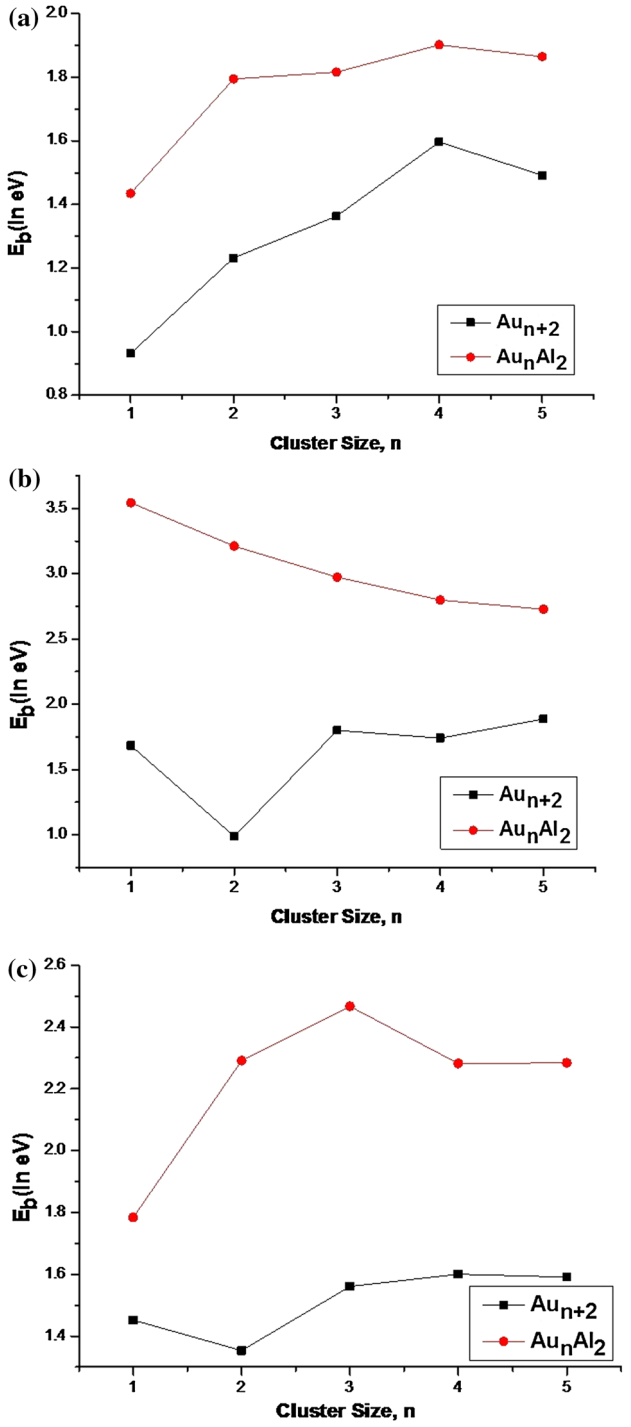

Fig. 4 Variation of binding energies with respect to cluster size for **a** neutral, **b** cationic and **c** anionic clusters in bare and aluminium-doped gold clusters

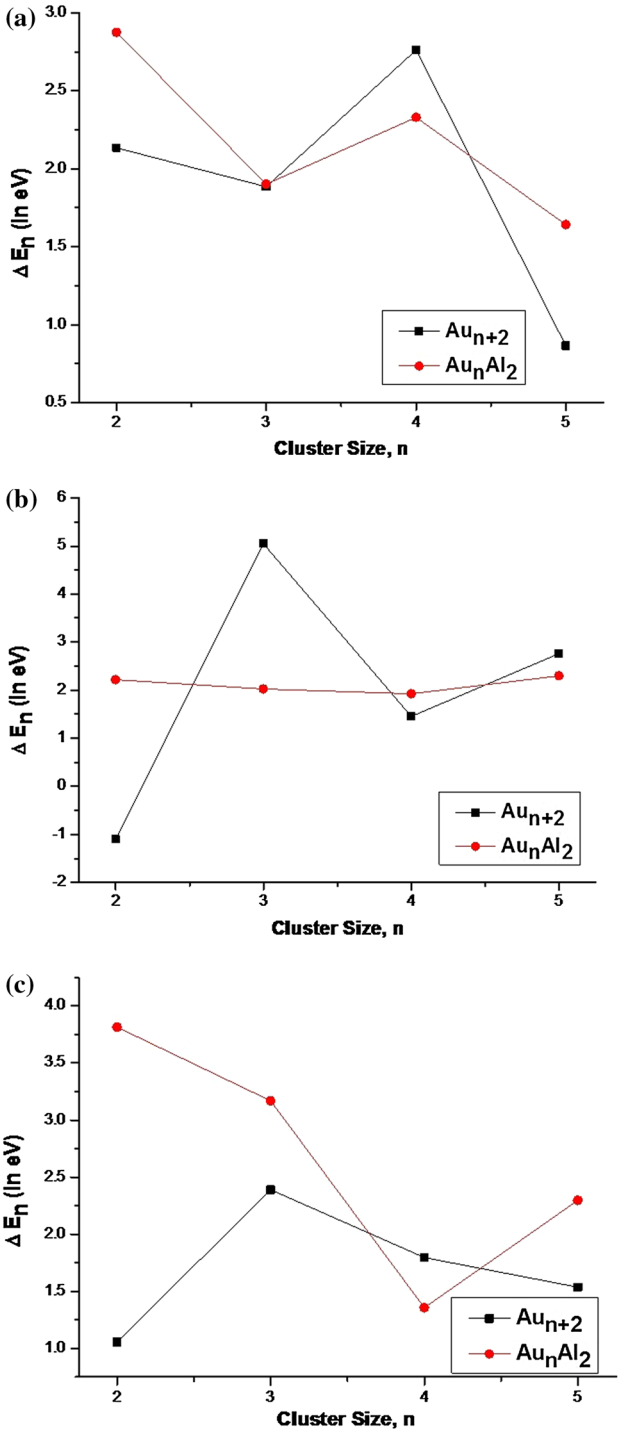

Fig. 5 Variation of fragmentation energies with respect to cluster size for **a** neutral, **b** cationic and **c** anionic clusters in bare and aluminium-doped gold clusters

Ionization potential and electron affinity

In cluster science, ionization potential and electron affinity are the two most important characteristics reflecting the electronic structure dependence relationship on size. Therefore, with the help of the same level of theory, we have calculated the vertical electron affinity (VEA) vertical ionization potential (VIP) and adiabatic ionization potential (AIP) values of the pure and doped clusters.

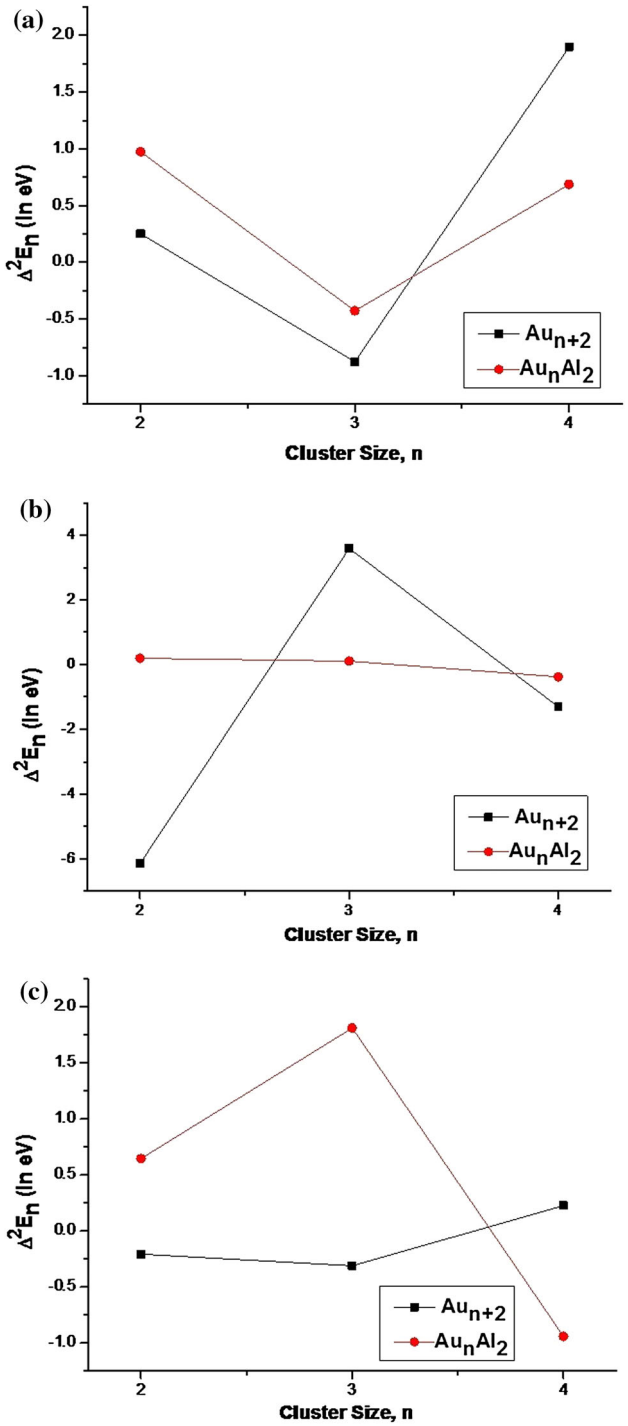

Fig. 6 Variation of second-order difference of energies with respect to cluster size for **a** neutral, **b** cationic and **c** anionic clusters in bare and aluminium-doped gold clusters

VEA measures the energy difference between the neutral and the anion clusters when the anion is at the optimized geometry of the neutral cluster. Thus,

$$\text{VEA} = E_{(\text{optimized neutral})} - E_{(\text{anion at optimized neutral geometry})} \quad (8)$$

Table 1 Vertical electron affinities of neutral Au_{n+2} and Au_nAl_2 clusters ($n = 1$–5)

	Au_{n+2}		Au_nAl_2
n	VEA (eV)	Experimental [48]	VEA (eV)
1	3.56	3.88	1.13
2	2.48	2.75	1.40
3	2.99	3.09	2.23
4	2.02	2.13	1.86
5	2.69	3.46	2.44

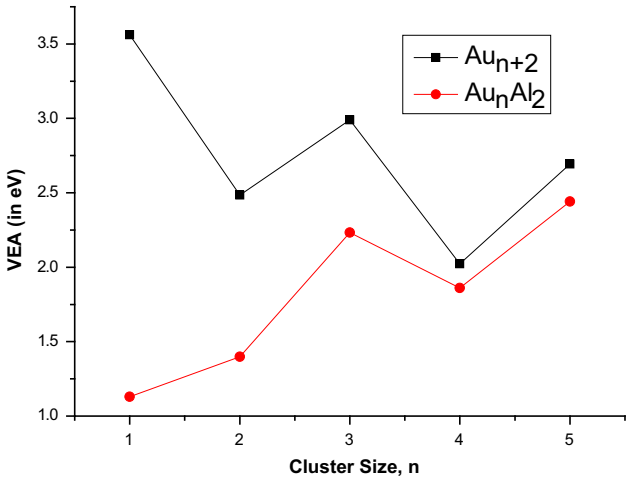

Fig. 7 Variation of VEA values with respect to cluster size for pure- and Al-doped Au clusters

Ionization potential (IP) is also an important parameter in describing the electronic property. It measures the energy difference between the ground state of the neutral and the ionized clusters. If the ionized cluster has the same geometry as the ground state of the neutral, the ionization energy corresponds to the VIP. On the other hand, the energy difference between the ground state of the cation and ground state of the neutral is referred to as the AIP. VIP is generally calculated using the following formula

$$\text{VIP} = E_{(\text{cation at optimized neutral geometry})} - E_{(\text{optimized neutral})} \quad (9)$$

Similarly, AIP is calculated as

$$\text{AIP} = E_{(\text{optimized cation})} - E_{(\text{optimized neutral})} \quad (10)$$

The calculated VEA values for the pure- and Al-doped clusters are listed in Table 1. The values are in the range 2.02–3.56 eV for the pure clusters and 1.13–2.44 eV for the doped clusters. The values obtained for Au_n clusters are in the close range of previous experimental results [48]. The plot of VEA against cluster size is depicted in Fig. 7. From the figure, we can see that the values of VEA for each cluster show an obvious oscillating behaviour with the

Table 2 Vertical and adiabatic ionization potentials of neutral Au_{n+2} and Au_nAl_2 clusters ($n = 1$–5)

	Au_{n+2}			Au_nAl_2	
n	VIP (eV)	AIP (eV)	Experimental [49]	VIP (eV)	AIP (eV)
1	6.99	6.99	7.27	5.87	5.87
2	7.81	10.20	8.60	6.54	6.54
3	7.06	7.06	7.61	5.75	6.41
4	8.38	8.38	8.80	6.50	6.82
5	6.48	6.48	7.80	6.18	6.16

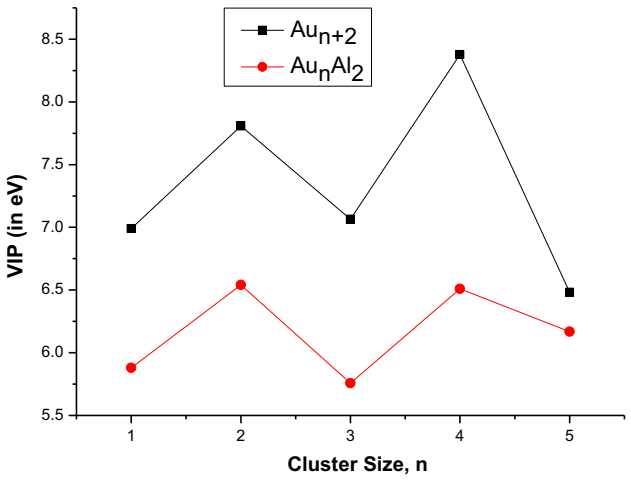

Fig. 8 Variation of VIP values with respect to cluster size for pure- and Al-doped Au clusters

increasing cluster size. The even number clusters have lower VEA values compared to the odd ones and hence are most stable. The VEA values for the doped clusters also have low VEA values indicating that they are more stable than the pure clusters. The variation of VEA with cluster size for our reported clusters seems to be identical with the previous study [30] as well. We are not able to compare the VEA values of Au_nAl_2 clusters due to lack of experimental values.

The calculated VIP and AIP values for Au_n and Au_nAl_2 clusters are listed in Table 2. The values obtained for Au_n clusters are in the range 6.48–8.48 eV which agrees well with the previous experimental results [49]. We are not able to make direct comparison on the doped clusters due to the lack of previous results. The VIP values with respect to cluster size show an even–odd alternation (Fig. 8) with lower values for odd-numbered clusters. Thus, these clusters are less stable than the even-numbered clusters.

From the above calculations, one can see that VIP values are larger than the VEA values for all the clusters. Hence these clusters can easily accept electrons.

QTAIM analysis

Using Bader's QTAIM [42–44], we have studied the topology of electron density of the clusters. This theory is mainly based on the three-dimensional electron density functions, $\rho(r)$. The topological analysis is the investigation of critical points of this function, $\rho(r)$. The commonly used parameters to ascertain the nature and extent of bonding between two atoms are the electron density, ρ and the Laplacian of electron density, $\nabla^2\rho$ at the bond critical point (BCP). Generally, a large value of $\rho(r)$ (> 0.2 au) and large and negative value of $\nabla^2\rho$ indicate a covalent or open-shell interaction, whereas a small value of $\rho(r)$ (< 0.10 au) and a positive value of $\nabla^2\rho$ indicate an ionic or closed shell interaction. However, we cannot extend this theory to transition metal complexes since the electron distribution of these elements is diffuse in nature. Hence, in transition metal complexes, the rule is changed and it is generally observed that ρ has a small value and $\nabla^2\rho$ has a small and positive value for a covalent interaction [50]. In addition to these two parameters, additional two parameters are also used to describe the bonding nature more appropriately. These two parameters are local electronic energy density function, $H(r)$ and relative kinetic energy density, $G(r)/\rho$, where, $H(r)$ is the sum of local kinetic $G(r)$ and potential $V(r)$ energy densities, i.e., $H(r) = G(r) + V(r)$. According to Cremer and Kraka [51], a value of $H(r) < 0$ at the BCP indicates the presence of significant covalent character or an open-shell interaction and lowering of potential energy of electrons at the BCP, whereas a value of $H(r) > 0$ at the BCP generally refers to a closed shell interaction, i.e., ionic, van der Waals, or hydrogen bonding. Similarly, value of $G(r)/\rho < 1$ at the BCP indicates a covalent interaction, whereas $G(r)/q > 1$ indicates the ionic nature of the bond [52].

The presence of BCP in all the studied clusters indicates the interaction between the Au and Al atoms. Only the most stable isomers that are found during geometry optimization are considered in QTAIM analysis. Our main aim of this QTAIM study was to notice the type of bond involves and the variation of bonding on doping Al in Au clusters. The values of the four different parameters that we observed during QTAIM are given in Table 3 for some selected clusters. The values for the remaining clusters are provided in Table S1 of supplementary information. The small and positive values obtained for ρ and $\nabla^2\rho$ for the structures in Table 3 reveal the covalent interaction between Au–Au and Au–Al atoms. Compared to that of Au–Au bond, BCP shifts toward Al atom in Au–Al bond as shown in Fig. S2 of supplementary information. As seen from Table 3, the $\rho(r)$ and $\nabla^2\rho(r)$ values for the doped clusters are smaller than that of the pure clusters indicating that extent of covalency is stronger in the doped clusters.

Table 3 Electron density, $\rho(r)$, Laplacian of electron density, $\nabla^2\rho(r)$, local electronic energy density function, $H(r)$ and relative kinetic energy density, $G(r)/\rho$ at the bond critical points (BCP) for some selected clusters

Cluster	Interaction	$\rho(r)$	$\nabla^2\rho(r)$	$H(r)$	$G(r)/\rho$
Neutral					
Au_3	Au_1–Au_2	0.06	0.15	−0.02	0.92
	Au_1–Au_3	0.06	0.15	−0.02	0.92
Au_4	Au_2–Au_4	0.06	0.15	−0.02	0.926
	Au_1–Au_2	0.05	0.12	−0.02	0.856
	Au_2–Au_3	0.05	0.12	−0.02	0.856
	Au_1–Au_4	0.05	0.12	−0.02	0.856
	Au_3–Au_4	0.05	0.12	−0.02	0.856
$AuAl_2$	Au_1–Al_2	0.04	0.06	−0.01	0.63
	Au_1–Al_3	0.04	0.06	−0.01	0.63
Au_2Al_2	Au_1–Al_3	0.04	0.03	−0.01	0.48
	Au_2–Al_3	0.04	0.03	−0.01	0.48
	Au_1–Al_4	0.04	0.03	−0.01	0.48
	Au_2–Al_4	0.04	0.03	−0.01	0.48
Cationic					
Au_3	Au_1–Au_2	0.06	0.13	−0.02	0.86
	Au_1–Au_3	0.06	0.13	−0.02	0.86
	Au_2–Au_3	0.06	0.13	−0.02	0.86
Au_4	Au_2–Au_4	0.05	0.12	−0.02	0.86
	Au_1–Au_2	0.05	0.12	−0.02	0.85
	Au_2–Au_3	0.05	0.12	−0.02	0.85
	Au_1–Au_4	0.05	0.12	−0.02	0.85
	Au_3–Au_4	0.05	0.12	−0.02	0.85
$AuAl_2$	Au_1–Al_2	0.04	0.01	−0.01	0.43
	Au_1–Al_3	0.04	0.01	−0.01	0.43
Au_2Al_2	Au_1–Al_3	0.04	0.04	−0.01	0.54
	Au_2–Al_3	0.04	0.04	−0.01	0.54
	Au_1–Al_4	0.04	0.04	−0.01	0.54
	Au_2–Al_4	0.04	0.04	−0.01	0.54
Anionic					
Au_3	Au_1–Au_2	0.06	0.14	−0.02	0.89
	Au_1–Au_3	0.06	0.14	−0.02	0.89
Au_4	Au_2–Au_4	0.04	0.1	−0.01	0.85
	Au_1–Au_2	0.05	0.12	−0.01	0.87
	Au_2–Au_3	0.05	0.12	−0.01	0.87
	Au_1–Au_4	0.05	0.12	−0.01	0.87
	Au_3–Au_4	0.05	0.12	−0.01	0.87
$AuAl_2$	Au_1–Al_2	0.04	0.07	−0.01	0.7
	Au_1–Al_3	0.04	0.07	−0.01	0.7
Au_2Al_2	Au_1–Al_3	0.05	0.08	−0.01	0.72
	Au_2–Al_3	0.04	0.03	−0.01	0.52
	Au_2–Al_4	0.04	0.06	−0.01	0.66
	Al_3–Al_4	0.03	0.06	−0.01	0.24

For all the studied clusters, we also observed only negative values for $H(r)$ which also indicates the presence of covalent interaction although the order is not too high. The presence of covalent interaction was further supported by $G(r)/\rho$ values which are much smaller than 1 in all the clusters. For the doped clusters, the values of $G(r)/\rho$ are more smaller than 1 compared to the pure ones. Hence it points toward greater covalency in doped clusters. To further study the interaction between Au and Al atoms, we observed the basin paths of the clusters (Fig. 9) which clearly confirm the interaction between the Au–Au and Au–Al atoms. The presence of cyclic structures obtained during optimization is confirmed by the presence of ring critical points (RCP). For example, we obtained a cyclic structure containing several rings for neutral Au_6 cluster which is confirmed by the presence of four RCPs. The main outcomes from this QTAIM analysis are that the studied clusters mainly possess covalent characters which are higher for the doped clusters.

Natural charge analysis

Applying the same level of theory, we have analysed the variation of charge for doping Al atoms in Au clusters with the help of Mulliken atomic charge localization. The charge analysis indicates that Al atoms have positive charges (0.441 *e*), whereas that of gold has negative charges (−0.881 in neutral $AuAl_2$ cluster. Similarly, for the cationic $AuAl_2$ cluster, Al atoms possess positive charges (0.966) and Au atoms have negative charge (−0.932). For anionic $AuAl_2$ cluster, charges are 0.114 and −1.229 for Al and Au atoms, respectively. All these charge values confirm the transfer of charges from Al atom to Au atom which is due to the larger electronegativity of Au (2.54) as compared to Al (1.61). Also we have generated the HOMO–LUMO isosurfaces for neutral and charged Au_3 and $AuAl_2$ as shown in Fig. 10. The isosurfaces clearly reveal the formation of covalent bonds in both the cases and it supports the formation of covalent bond in accordance with our QTAIM study. However, the isosurfaces also indicate that on doping Al atoms, the bonding nature somewhat changes from pi(π) to sigma(σ).

Conclusions

In this manuscript, we have carried out a systematic study on the structures, stabilities, and electronic properties of small bare gold Au_n and doubly Al-doped Au_nAl_2 (neutral

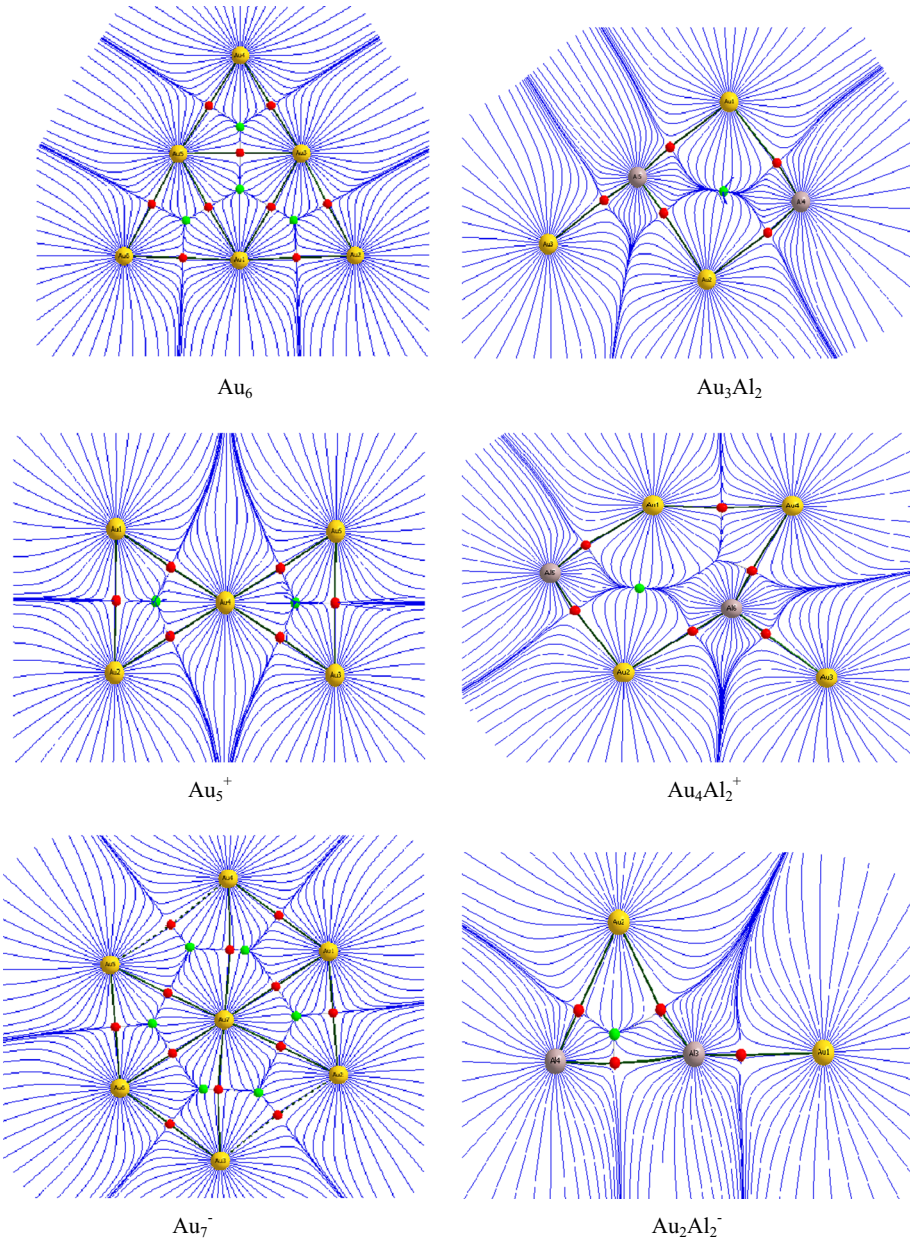

Fig. 9 Trajectory field in some of the Au_n and Au_nAl_2 clusters. Gold and aluminium atoms are represented by *yellow* and *grey* spheres, respectively. Bond paths and basin paths are indicated by *dark green* and *blue lines*, while the interatomic surfaces are indicated by *dark blue lines*. *Red* and *green dots* indicate bond critical points and ring critical points, respectively (Color figure online)

and charged) clusters using PW91PW91 level of theory. The main outcomes from this study are summarised as below:

1. All the neutral Al-doped Au_n clusters adopt planar structures. This is in contrast to single Al-doped clusters. The structures of doped clusters are different to that of pure clusters indicating the effect of doubly doped Al in the Au clusters. For the charged clusters, a deviation is observed at $n = 3$ and the doped clusters also have different geometries to that of pure clusters.
2. The relative stabilities of the pure and doped clusters are expressed in terms of binding energy per atom, fragmentation energies and second-order difference of energies. These curves follow even–odd oscillation. The binding energy plots clearly indicate the enhanced stability of the doped clusters compared to that of the pure ones. Among the doped clusters, Au_2Al_2, Au_4Al_2, $Au_2Al_2^+$ and $Au_3Al_2^-$ possess greater stability in the region $n = 1$–5.
3. The electronic properties are expressed in terms of IP and electron affinity. The calculated values for the clusters show excellent agreement with the previously reported experimental results. Hence our studied structures are accurate. These properties also indicate the electron-accepting tendency of the studied clusters.

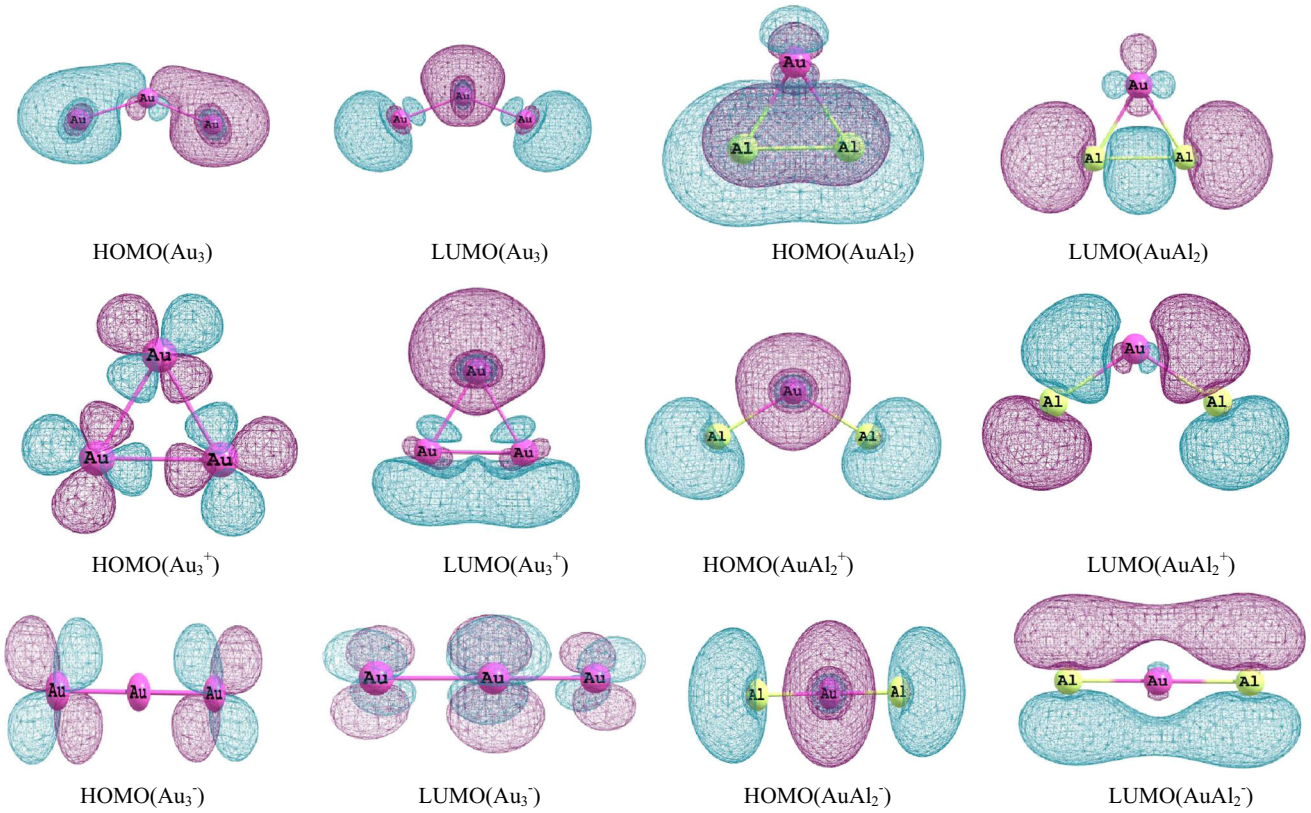

Fig. 10 HOMO and LUMO isosurfaces of Au_3 and $AuAl_2$ clusters

4. The bonding parameters described in terms of QTAIM study indicate the presence of covalent bond in the clusters. The electron density, ρ, and its Laplacian, $\nabla^2\rho$ at the Au–Au and Au–Al BCPs are found to be very small and positive. Also the local electronic energy density function, $H(r)$ and relative kinetic energy density, $G(r)/\rho$ values are characteristics of covalent character.
5. The natural charge analysis describes the transfer of electron from Al to Au atoms which results the enhance stability of the doped clusters. The HOMO–LUMO isosurface further supports the covalent behaviour of the clusters. Therefore, from all the present observations, we come to the conclusion that the doping of two Al atoms can effectively increase the stability of the Au clusters.

The detailed investigation into structures, stability and electronic properties of small bimetallic clusters in our present work can provide a strong support in understanding the larger-doped clusters of gold as well as other metals. Also we strongly believe that this work will provide powerful guidelines in further experimental research.

Acknowledgements The work is funded by the Department of Science and Technology, New Delhi in the form of a research project (SR/NM/NS-1023/2011-G). One of the authors, D.B. is thankful to CSIR, New Delhi for providing Senior Research fellowship.

References

1. Eachus RS, Marchetti AP, Muenter AA (1999) The photolysis of silver halide imaging materials. Annu Rev Phys Chem 50:117–144
2. Scaffardi LB, Pellegri N, Ode Sanctis, Tocho JO (2005) Sizing gold nanoparticles by optical extinction spectroscopy. Nanotechnology 16:158–163
3. Torres MB, Fernández EM, Balbás LC (2008) Theoretical study of oxygen adsorption on pure Au_{n+1}^+ and doped MAu_n^+ cationic gold clusters for M = Ti, Fe and n = 3–7. J Phys Chem A 112:6678–6689
4. Autschbach J, Hess BA, Johansson MP, Neugebauer J, Patzschke M, Pyykkö P, Reiher M, Sundholm D (2004) Properties of WAu_{12}. Phys Chem Chem Phys 6:11–22
5. Lopez N, Norskov JK (2002) Catalytic CO oxidation by a gold nanoparticle: a density functional study. J Am Chem Soc 124:11262–11263
6. Haruta M, Kobayashi T, Samo H, Yamada N (1987) Novel gold catalysts for the oxidation of carbon monoxide at a temperature far below 0 °C. Chem Lett 2:405–408
7. Deka RC, Bhattacharjee D, Chakrabartty AK, Mishra BK (2014) Catalytic oxidation of NO by Au_2^- dimers: a DFT study. RSC Adv 4:5399–5404
8. Chrétien SC, Buratto SK, Metiu H (2007) Catalysis by very small Au clusters. Curr Opin Solid State Mater Sci 11:62–75

9. Werner J (1999) Chemical aspects of the use of gold clusters in structural biology. J Struct Biol 127:106–112
10. Gaudry M, Lerme J, Cottancin E, Pellarin M, Vialle JL, Broyer M, Prevel B, Treilleux M, Melinon P (2001) Optical properties of $(Au_xAg_{1-x})_n$ clusters embedded in alumina: evolution with size and stoichiometry. Phys Rev B 64:085407
11. Manzoor D, Krishnamurty S, Pal S (2014) Effect of silicon doping on the reactivity and catalytic activity of gold clusters. J Phys Chem C 118:7501–7507
12. Liu P, Song K, Zhang D, Liu C (2012) A comparative theoretical study of the catalytic activities of Au_2^- and $AuAg^-$ dimers for CO oxidation. J Mol Model 18:1809–1818
13. Deka A, Deka RC (2008) Structural and electronic properties of stable Au_n (n = 2–13) clusters: a density functional study. J Mol Struct (Theochem) 870:83–93
14. Viswanathan M, Sankaran B (2006) A DFT study of the electronic property of gold nanoclusters (Au_x, x = 1–12 atoms). Bull Catal Soc India 5:26–32
15. Shao P, Kuang XY, Zhao YR, Li YF, Wang SJ (2012) Equilibrium geometries, stabilities, and electronic properties of the cationic Au_nBe^+ (n = 1–8) clusters: comparison with pure gold clusters. J Mol Model 18:3553–3562
16. Shao N, Huang W, Mei WN, Wang LS, Wu Q, Zeng XC (2014) Structural evolution of medium-sized gold clusters Au_n^- (n = 36, 37, 38): appearance of bulk-like face centered cubic fragment. J Phys Chem C 118:6887–6892
17. Pal R, Wang LM, Huang W, Wang LS, Zeng XC (2009) Structural evolution of doped gold clusters: MAu_x^- (M = Si, Ge, Sn; x = 5–8). J Am Chem Soc 131:3396
18. Zhang M, Feng XJ, Zhao LX, He LM, Luo YH (2010) Density-functional investigation of 3d, 4d, 5d impurity doped Au_6 clusters. Chin Phys B 19:043103
19. Lu P, Liu GH, Kuang XY (2014) Probing the structural and electronic properties of bimetallic chromium–gold clusters Cr_mAu_n (m + n ≤ 6): comparison with pure chromium and gold clusters. J Mol Model 20:2385
20. Tafoughalt MA, Sarmah M (2012) Density functional investigation of structural and electronic properties of small bimetallic silver–gold clusters. Phys B 407:2014–2024
21. Soto JR, Molinaa B, Castro JJ (2014) Nonadiabatic structure instability of planar hexagonal gold cluster cation Au_7 and its spectral signature. RSC Adv 4:8157–8164
22. Li YF, Kuang XY, Wang SJ, Zhao YR (2010) Geometries, stabilities, and electronic properties of small anion Mg-doped gold clusters: a density functional theory study. J Phys Chem A 114:11691–11698
23. Wang HQ, Kuang XY, Li HF (2010) Density functional study of structural and electronic properties of bimetallic copper–gold clusters: comparison with pure and doped gold clusters. Phys Chem Chem Phys 12:5156–5165
24. Koyasu K, Naono Y, Akutsu M, Mitsui M, Nakajima A (2006) Photoelectron spectroscopy of binary Au cluster anions with a doped metal atom: Au_nM^- (n = 2–7), M = Pd, Ni, Zn, Cu, and Mg. Chem Phys Lett 422:62–66
25. Guo JJ, Yang JX, Die D (2008) Ab initio study of small Au_nY_2 (n = 1–4) clusters. Phys B 403:4033–4037
26. Bhattacharjee D, Mishra BK, Chakrabartty AK, Deka RC (2014) DFT and QTAIM studies on structure and stability of beryllium doped gold clusters. Comput Theor Chem 1034:61–72
27. Bouwen W, Vanhoutte F, Despa F, Bouckaert S, Neukermans S, Kuhn LT, Weidele H, Lievens P, Silverans RE (1999) Stability effects of Au_nX_m (X = Cu, Al, Y, In) clusters. Chem Phys Lett 314:227–233
28. Heinebrodt M, Malinowski N, Tast F, Branz W, Billas IML, Martin TP (1999) Bonding character of bimetallic clusters AuX (X = Al, In, Cs). J Chem Phys 110:9915–9921
29. Wang CJ, Kuang XY, Wang HQ, Li HF, Gu JB, Liu J (2012) Density-functional investigation of the geometries, stabilities, electronic, and magnetic properties of gold cluster anions doped with aluminum: Au_nAl^- ($1 \le n \le 8$). Comput Theor Chem 1002:31–36
30. Zhao LX, Feng XJ, Cao TT, Liang X, Luo YH (2009) Density functional study of Al doped Au clusters. Chin Phys B 18:2709–2718
31. Majumder C, Kandalam AK, Jena P (2006) Structure and bonding of Au_5M (M = Na, Mg, Al, Si, P, and S) clusters. Phys Rev B 74:205437
32. Accelrys Material Studio 7.0
33. Rappé AK, Casewit CJ, Colwell KS, Goddard WA III, Skiff WM (1992) UFF, a full periodic table force field for molecular mechanics and molecular dynamics simulations. J Am Chem Soc 114:10024–10035
34. Antonello S, Arrigoni G, Dainese T, Nardi MD, Parisio G, Perotti L, René A, Venzo A, Maran F (2014) Electron transfer through 3D monolayers on Au_{25} clusters. ACS Nano 8:2788–2795
35. Huber SE, Warakulwit C, Limtrakul J, Tsukudad T, Probst M (2012) Thermal stabilization of thin gold nanowires by surfactant-coating: a molecular dynamics study. Nanoscale 4:585–590
36. Perdew P, Chevary JA, Vosko SH, Jackson KA, Pederson MR, Singh DJ, Fiolhais C (1992) Atoms, molecules, solids, and surfaces: applications of the generalized gradient approximation for exchange and correlation. Phys Rev B 46:6671
37. Hay PJ, Wadt WR (1985) Ab initio effective core potentials for molecular calculations. Potentials for the transition metal atoms Sc to Hg. J Chem Phys 82:270–283
38. Hay PJ, Wadt WR (1985) Ab initio effective core potentials for molecular calculations. Potentials for K to Au including the outermost core orbitals. J Chem Phys 82:299–310
39. Xie H, Li X, Zhao L, Qin Z, Wu X, Tang Z, Xing X (2012) Photoelectron imaging and theoretical calculations of bimetallic clusters: $AgCu^-$, $AgCu_2^{(-)}$, and Ag_2Cu^-. J Phys Chem A 116:10365–10370
40. Zhou J, Li ZH, Wang WN, Fan KN (2006) Density functional study of the interaction of carbon monoxide with small neutral and charged silver clusters. J Phys Chem A 110:7167–7172
41. Frisch MJ, Trucks GW, Schlegel HB, Scuseria GE, Robb MA, Cheeseman JR, Scalmani G, Barone V, Mennucci B, Petersson GA, Nakatsuji H, Caricato M, Li X, Hratchian HP, Izmaylov AF, Bloino J, Zheng G, Sonnenberg JL, Hada M, Ehara M, Toyota K, Fukuda R, Hasegawa J, Ishida M, Nakajima T, Honda Y, Kitao O, Nakai H, Vreven T, Montgomery JA Jr, Peralta JE, Ogliaro F, Bearpark M, Heyd JJ, Brothers E, Kudin KN, Staroverov VN, Kobayashi R, Normand J, Raghavachari K, Rendell K, Burant JC, Iyengar SS, Tomasi J, Cossi M, Rega N, Millam JM, Klene M, Knox JE, Cross JB, Bakken V, Adamo C, Jaramillo J, Gomperts R, Stratmann RE, Yazyev O, Austin AJ, Cammi R, Pomelli C, Ochterski JW, Martin RL, Morokuma K, Zakrzewski VG, Voth GA, Salvador P, Dannenberg JJ, Dapprich S, Daniels AD, Farkas O, Foresman JB, Ortiz JV, Cioslowski J, Fox DJ (2010) Gaussian 09, revision B.01. Gaussian Inc, Wallingford
42. Bader RFW (1990) Atoms in molecules: a quantum theory. Oxford University Press, Oxford
43. Bader RFW (1998) A bond path: a universal indicator of bonded interactions. J Phys Chem A 102:7314–7323
44. Bader RFW (1991) A quantum theory of molecular structure and its applications. Chem Rev 91:893
45. Keith TA (2013) AIMAll (version 13.02.26). TK Gristmill Software, Overland Park (aim.tkgristmill.com)
46. Li YF, Mao AJ, Li Y, Kuang XY (2012) Density functional study on size-dependent structures, stabilities, electronic and magnetic properties of Au_nM (M = Al and Si, n = 1–9) clusters: comparison with pure gold clusters. J Mol Model 18:3061–3072

47. Bhattacharjee D, Mishra BK, Deka RC (2014) A DFT study on structure, stabilities and electronic properties of double magnesium doped gold clusters. RSC Adv 4:56571–56581
48. Hakkinen H, Yoon B, Landman U, Li X, Zhai HJ, Wang LS (2003) On the electronic and atomic structures of small Au_N^- (N = 4–14) clusters: a photoelectron spectroscopy and density-functional study. J Phys Chem A 107:6168–6175
49. Cheeseman MA, Eyler JR (1992) Ionization potentials and reactivity of coinage metal clusters. J Phys Chem 96:1082–1087
50. Farrugia LJ, Evans C, Tegel MJ (2006) Chemical bonds without "Chemical Bonding"? A combined experimental and theoretical charge density study on an iron trimethylenemethane complex. J Phys Chem A 110:7952–7961
51. Cremer D, Kraka E (1984) Chemical bonds without bonding electron density-does the difference electron-density analysis suffice for a description of the chemical bond? Angew Chem Int Ed 23:627–628
52. Macchi P, Sironi A (2003) Chemical bonding in transition metal carbonyl clusters: complementary analysis of theoretical and experimental electron densities. Coord Chem Rev 238–239: 383–412